Hygroscopic behavior and chemical composition evolution of internally mixed aerosols composed of oxalic acid and ammonium sulfate

Xiaowei Wang[1,2], Bo Jing[3], Fang Tan[3,4], Jiabi Ma[1], Yunhong Zhang[1] and Maofa Ge[3,4,5]

[1]The Institute of Chemical Physics, School of Chemistry and Chemical Engineering, Beijing Institute of Technology, Beijing 100081, P. R. China

[2]School of Chemical Engineering and Pharmaceutics, Henan University of Science and Technology, Luoyang 471023, P. R. China

[3]Beijing National Laboratory for Molecular Sciences (BNLMS), State Key Laboratory for Structural Chemistry of Unstable and Stable Species, CAS Research/Education Center for Excellence in Molecular Sciences, Institute of Chemistry, Chinese Academy of Sciences, Beijing 100190, P. R. China

[4]University of Chinese Academy of Sciences, Beijing 100049, P. R. China

[5]Center for Excellence in Regional Atmospheric Environment, Institute of Urban Environment, Chinese Academy of Sciences, Xiamen 361021, P. R. China

Correspondence to: Yunhong Zhang (yhz@bit.edu.cn) and Maofa Ge (gemaofa@iccas.ac.cn)

Abstract

Although water uptake of aerosols plays an important role in the atmospheric environment, the effects of interactions between components on chemical composition and hygroscopicity of aerosols are still not well constrained. The hygroscopic properties and phase transformation of oxalic acid (OA) and mixed particles composed of ammonium sulfate (AS) and OA with different organic to inorganic molar ratios (OIRs) have been investigated by using confocal Raman spectroscopy. It is found that OA droplets first crystallize to form oxalic acid dihydrate at 77% relative humidity (RH), and further lose crystalline water to convert into anhydrous oxalic acid around 5% RH during the dehydration process. The deliquescence and efflorescence point for AS is determined to be 80.1 ± 1.5% RH and 44.3 ± 2.5% RH, respectively. The observed efflorescence relative humidity (ERH) for mixed OA/AS droplets with OIRs of 1:3, 1:1 and 3:1 is 34.4 ± 2.0% RH, 44.3 ± 2.5% RH and 64.4 ± 3.0% RH, respectively, indicating the elevated OA content appears to favor the crystallization of mixed systems at higher RH. However, the partial deliquescence relative humidity (DRH) for mixed OA/AS particles with OIR of 1:3 and 1:1 is observed to occur at 81.1 ± 1.5% RH and 77 ± 1.0% RH, respectively. The Raman spectra of mixed OA/AS droplets indicate the formation of ammonium hydrogen oxalate ($NH_4HC_2O_4$) and ammonium hydrogen sulfate

Atmospheric
Chemistry
and Physics

Discussions

1   (NH₄HSO₄) from interactions between OA and AS in aerosols after slow dehydration process in the

2   time scale of hours, which considerably influence the subsequent deliquescence behavior of

3   internally mixed particles with different OIRs. The mixed OA/AS particles with 3:1 ratio exhibit no

4   deliquescence transition over the RH range studied due to the considerable transformation of

5   $(NH_4)_2SO_4$ into nonhygroscopic $NH_4HC_2O_4$. Although the hygroscopic growth of mixed OA/AS

6   droplets is comparable to that of AS or OA at high RH during the dehydration process, Raman

7   growth factors of mixed particles after deliquescence are substantially lower than those of mixed

8   OA/AS droplets during the efflorescence process and further decrease with elevated OA content.

9   The discrepancies for Raman growth factors of mixed OA/AS particles between the dehydration

10 and hydration process at high RH can be attributed to the significant formation of $NH_4HC_2O_4$ and

11 residual OA, which remain solid at high RH and thus result in less water uptake of mixed particles.

12 These findings improve the understanding of the role of reactions between dicarboxylic acid and

13 inorganic salt in the chemical and physical properties of aerosol particles, and might have important

14 implications for atmospheric chemistry.

1 Introduction

16 Atmospheric aerosols have vital impacts on the Earth's climate directly by scattering, reflecting and

17 absorbing solar radiation, and indirectly by influencing formation of clouds and precipitation (Tang

18 and Munkelwitz, 1994b; Jacobson et al., 2000; Penner et al., 2001; Pöschl, 2005; Martin, 2000; Von

19 Schneidemesser et al., 2015). Direct and indirect effects depend on the chemical and physical

20 properties of atmospheric aerosols, including size, structure, hygroscopicity and chemical

21 composition. Field observations indicate that aerosol particles are generally internal mixtures of

22 inorganic and organic compounds in the atmosphere (Saxena et al., 1995; Murphy et al., 1998;

23 Murphy et al., 2006; Pratt and Prather, 2010). Ammonium sulfate (AS) is one of the most abundant

24 inorganic constituents in the atmosphere, hygroscopicity of which has been widely investigated (Liu

25 et al., 2008; Cziczo et al., 1997; Laskina et al., 2015).

26 Oxalic acid (OA) is ubiquitous and has been identified as the dominant dicarboxylic acid in urban

27 and remote atmospheric aerosols (Chebbi and Carlier, 1996; Kanakidou et al., 2004; Yang and Yu,

28 2008; Wang et al., 2012; Kawamura and Bikkina, 2016). Previous studies have focused on

29 deliquescence behavior of pure OA (Peng et al., 2001; Braban et al., 2003; Miñambres et al., 2013;

30 Ma et al., 2013a; Jing et al., 2016). It was found that due to its high deliquescence point OA

1   exhibited no deliquescence transition or hygroscopic growth within relative humidity (RH) range

2   studied by an electrodynamic balance (EDB) (Peng et al., 2001), vapor sorption analyzer (Ma et al.,

3   2013a) or hygroscopicity tandem differential mobility analyzer (HTDMA) (Jing et al., 2016).

4   Braban et al. (2003) reported that OA could deliquesce at 98% RH using aerosol flow tube Fourier

5   transform infrared spectroscopy (AFT-FTIR). However, the study on the efflorescence behavior of

6   OA during the dehydration process remains limited (Peng et al., 2001; Mikhailov et al., 2009). Peng

7   et al. (2001) observed the efflorescence transition of OA using EDB while Mikhailov et al. (2009)

8   reported continuous hygroscopic growth of OA during both hydration and dehydration process

9   using the HTDMA.

10   The dicarboxylic acids can affect properties of internally mixed aerosol particles such as

11   hygroscopicity, phase transition, solubility and chemical reactivity (Lightstone et al., 2000; Brooks

12   et al., 2002; Sjogren et al., 2007; Kumar et al., 2003; Treuel et al., 2011; Laskin et al., 2012; Drozd

13   et al., 2014; Peng et al., 2016; Jing et al., 2016; Li et al., 2017; Jing et al., 2017). Field

14   measurements have observed the formation of low-volatility organic salts in atmospheric particles

15   due to the reactions of organic acids with mineral salts, chloride salts, nitrate salts, ammonium and

16   amines. The organic salts formed typically have varying hygroscopicity compared to the

17   corresponding organic acids. Thus, these drastic changes in aerosol composition have potential

18   impacts on the water uptake and related physicochemical properties of particles. The effects of OA

19   on deliquescence behaviors of AS have been extensively investigated (Brooks et al., 2002; Prenni et

20   al., 2003; Wise et al., 2003; Miñambres et al., 2013; Jing et al., 2016). The majority of studies found

21   that the presence of OA had no obvious impacts on the deliquescence process of OA/AS mixtures

22   with minor OA content (Brooks et al., 2002; Prenni et al., 2003; Wise et al., 2003). To our

23   knowledge, there is still a lack of studies on the efflorescence process of OA/AS mixed systems. In

24   fact, the efflorescence behavior is a critical hygroscopic characteristic of atmospheric aerosols,

25   which may favor specific chemical interactions between components within the supersaturated

26   droplets. For example, previous studies have found that the chloride depletion could occur in the

27   NaCl/dicarboxylic acids mixed aerosols during the dehydration or efflorescence process, which led

28   to the formation of organic salts and in turn affected subsequent deliquescence behaviors of aerosols

29   (Laskin et al., 2012; Ghorai et al., 2014). Oxalic acid has been found to react with both mono- and

30   di-valent cations to form low volatility and solubility compounds (Drozd et al., 2014). Miñambres

Atmospheric
Chemistry
and Physics
Discussions

1   et al. (2013) proposed that OA might react with AS to form ammonium hydrogen oxalate and

2   ammonium hydrogen sulfate within OA/AS solution. It merits further investigation on the

3   interactions between OA and AS and related influence on the water uptake behaviors of aerosols

4   during the dehydration and hydration processes.

5   Raman spectroscopy is a powerful technique to characterize aerosol compositions, water contents,

6   molecular interactions, and particle phases especially for the efflorescence process (Ma and He,

7   2012; Laskina et al., 2013; Ma et al., 2013b; Yu et al., 2012; Zhou et al., 2014; Wang et al., 2015).

8   In this study, the phase transformations and hygroscopic properties of OA and mixed OA/AS

9   droplets with varying OA content were studied by confocal Raman spectroscopy in conjunction

10 with optical microscopy. Furthermore, we explored the effects of reactions between OA and AS on

11 the chemical compositions and hygroscopic properties of mixed OA/AS droplets.

12 **2 Experimental section**

13 **2.1 Sample preparation**

14 Ammonium sulfate (AS) and oxalic acid dihydrate were purchased from Sinopharm Chemical

15 Reagent Co. Ltd. (99.0% purity) and used without further purification. The 0.5 mol L^{-1} pure

16 component AS and OA solutions were prepared by dissolving AS and oxalic acid dihydrate in

17 ultrapure water (18.2 MΩ·cm, Barnstead Easypure II), respectively. The mixed OA/AS solutions

18 with different organic to inorganic molar ratios (OIRs) of 1:3, 1:1 and 3:1 were obtained by

19 dissolving a designated amount of OA into AS solutions. Using a syringe, droplets from the

20 solutions were injected onto the polytetrafluorethylene (PTFE) film fixed to the bottom of the

21 sample cell. The diameters of these droplets ranged from 30 to 40 μm at ~ 95% RH. Then, the

22 sample cell was sealed by a transparent polyethylene film and the RH in the sample cell was

23 regulated by nitrogen streams consisting of a mixture of water-saturated N_2 and dry N_2 at controlled

24 flow rates. The RH and temperature of the outflow from the sample cell was measured by a

25 humidity/temperature meter (Centertek Center 313) with an accuracy of $\pm 2.5\%$ and ± 0.7 K placed

26 near the exit of the sample cell.

27 **2.2 Apparatus and conditions for the measurements**

28 The experimental setup used in this study was described in detail in previous work (Wang et al.,

29 2008; Dong et al., 2009; Zhou et al., 2014). Briefly, the Renishaw InVia confocal Raman

Atmospheric
Chemistry
and Physics
Discussions

1   spectrometer equipped with a Leica DMLM microscope was used to acquire the Raman spectra. An

2   argon-ion laser (wavelength 514.5 nm, model Stellar-REN, Modu-Laser) was used as an excitation

3   source with an output power of 20 mW, and a 514.5 nm notch filter was adopted to remove the

4   strong Rayleigh scattering. An 1800 g mm^{-1} grating was used to obtain the spectra in the range of

5   200-4000 cm^{-1} with a resolution of about 1 cm^{-1}. Spectral calibration was made using the 520 ± 0.05

6   cm^{-1} Stokes shift of silicon band before performing measurements. Then, spectroscopic

7   measurements were made on droplets observed by using the Leica DMLM microscope with a $50\times$

8   objective lens. The spectra were obtained with three spectral scans, and each time with an

9   accumulation time of 10 s. The sample droplets were injected onto the substrate at high RH (~ 95%

10   RH). Subsequently, the RH was decreased stepwise for dehydration process, and increased from RH

11   < 3% to high RH for hydration process. The particles were equilibrated with water vapor at a given

12   RH for about 40 min. The spectra of AS, OA and mixed OA/AS droplets were monitored and

13   measured through a full humidity cycle. Each humidity cycle experiment was repeated at least three

14   times. All the measurements were taken at ambient temperature of about 297 K.

15   Raman growth factor is defined as the ratio of integrated area of OH stretching mode of water

16   (3350−3700 cm^{-1}) at each RH (A_{RH}) normalized to that of a dry particle (A_{RH0}) according to Eq. (1)

17   (Laskina et al., 2015).

18   $$g_{RH} = A_{RH}/A_{RH0} \qquad\qquad (1)$$

19   where A_{RH} is integrated area of OH stretching mode from water (3350-3700 cm^{-1}) at a specific RH

20   and A_{RH0} is that of a dry particle. Hygroscopic growth curves are acquired by plotting the Raman

21   growth factor as a function of RH.

22   **3 Results and discussion**

23   **3.1 Raman spectra of pure AS and OA droplets**

24   The Raman spectra of AS droplets during the dehydration and hydration process as a function of

25   RH can be found in Fig. S1 (a) and (b) in the Supplement, respectively. AS droplets effloresce at

26   $44.3 \pm 2.5\%$ RH, as indicated by the disappearance of the water peak centered at 3437 cm^{-1} and a

27   red-shift in $\nu_s(SO_4^{2-})$ peak position from 979 to 974 cm^{-1} during the dehydration process. For the

28   hydration process, the deliquescence of AS particles is observed to occur at $80.1 \pm 1.5\%$ RH,

29   resulting in an abrupt increase in the absorbance of the water peak centered at 3437 cm^{-1} and a

30   blue-shift in $\nu_s(SO_4^{2-})$ peak position from 974 to 979 cm^{-1}.

1   The Raman spectra of OA droplets with varying RH during the dehydration and hydration

2   process are shown in Fig. 1, and the assignments of the peaks for OA are presented in Table 1

3   according to previous studies (Hibben, 1935; Ebisuzaki and Angel, 1981; Chang and Huang, 1997;

4   Mohaček-Grošev et al., 2009; Ma et al., 2013a). As seen in Fig. 1a, the feature bands for OA

5   droplets are observed at 457, 845, 1460, 1636, 1750 and 3433 cm^{-1} at 92.5% RH. At lower RH

6   around 77% (Fig. 1a, magenta line), these bands shift to 477, 855, 1490, 1627, 1737, 3433 and 3474

7   cm^{-1}, and a new band at 1689 cm^{-1} occurs, which is entirely consistent with the spectrum of oxalic

8   acid dihydrate (Fig. 1a, black line). It indicates OA droplets crystallize to form oxalic acid dihydrate.

9   As RH further decreases to ~5.0%, the peaks shift to 482, 828, 845, 1477, 1710, 2587, 2760 and

10   2909 cm^{-1}, and peaks at 3433 and 3474 cm^{-1} assigned to v(OH) vanish, which is the spectrum

11   feature of anhydrous oxalic acid. This result implies that oxalic acid dihydrate is converted to

12   anhydrous oxalic acid in the RH around 5.0%. The Raman spectra of anhydrous oxalic acid

13   particles during the hydration process as a function of RH are shown in Fig. 1b. It can be found that

14   the Raman spectra feature for anhydrous oxalic acid particles occurs at RH<19.6%. At 19.6% RH,

15   the peaks observed at 477, 855, 1490, 1627, 1690, 1737, 3433 and 3474 cm^{-1} are identical to that of

16   oxalic acid dihydrate (Fig. 1a, black line), indicating the formation of oxalic acid dihydrate. The

17   observation of no spectral change until 94% RH suggests that oxalic acid dihydrate shows no

18   deliquescence transition in the 0-94 % RH range studied, consistent with previous studies (Peng et

19   al., 2001; Braban et al., 2003; Ma et al., 2013a; Jing et al., 2016). The transition point of anhydrous

20   oxalic acid to oxalic acid dihydrate upon hydration is 17.9-19.6% (Fig. 1b), in agreement with the

21   results reported by Braban et al. (2003) and Ma et al. (2013a).

22   **3.2 Raman spectra of OA/AS mixtures**

23   The Raman spectra of mixed OA/AS droplets with OIRs of 1:3, 1:1 and 3:1 at various RHs during

24   the dehydration process are depicted in Fig. 2. The corresponding spectra for hydration process are

25   given in Fig. S2 in the Supplement. The detailed assignments are summarized in Table 2. For the

26   mixed OA/AS droplets (OIR = 1:3) at 96.2% RH (seen in Fig. 2a), the bands at 450 and 979 cm^{-1}

27   are characteristic peaks of the sulfate ion, and peak at 1049 cm^{-1} are due to vibrating mode of

28   ($v_s(SO_3)$) of HSO_4^- ion. In addition, the peak at 1741 cm^{-1} can be assigned to vibrating mode of OA,

29   and peak at 1446 cm^{-1} can be attributed to vibrating mode of $HC_2O_4^-$ ion. With decreasing RH, only

30   small changes are observed in the spectra until the RH reaches 34.4% RH. At 34.4% RH, the shift

Atmospheric
Chemistry
and Physics
Discussions

1   of $v_s(SO_4^{2-})$ peak from 979 cm^{-1} to 974 cm^{-1} indicates the crystallization of AS. A new band

2   centered at 874 cm^{-1} corresponds to the vibrational mode (δ(S-OH)) of HSO$_4^-$ ion from NH$_4$HSO$_4$

3   and the HC$_2$O$_4^-$ ion vibrating (Irish and Chen, 1970; Dawson et al., 1986; Villepin and Novak, 1971;

4   Shippey, 1979), suggesting the formation of crystalline NH$_4$HSO$_4$ and NH$_4$HC$_2$O$_4$. Moreover, the

5   several new peaks at 1416, 1469 and 1660 cm^{-1} can be attributed to the HC$_2$O$_4^-$ ion vibrating of

6   crystalline NH$_4$HC$_2$O$_4$. Therefore, the evolution of Raman spectra of the mixed OA/AS droplets

7   (OIR = 1:3) during the dehydration process confirms that OA could react with AS to form

8   NH$_4$HSO$_4$ and NH$_4$HC$_2$O$_4$, which supports previous speculation for the reaction between OA and

9   AS (Miñambres et al., 2013). The reaction of OA with AS occurs via the following pathway:

10    $$(NH_4)_2SO_{4(aq)} + H_2C_2O_{4(aq)} = NH_4HSO_{4(aq)} + NH_4HC_2O_{4(aq)}$$
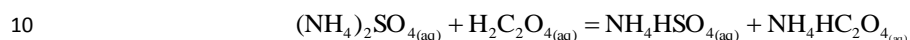
11   For the mixed OA/AS droplets (OIR = 1:1, Fig. 2b), the evolution of spectra shows resemblance

12   to that of mixed droplets (OIR = 1:3). At 96.1% RH, the bands at 450 and 979 cm^{-1} are

13   characteristic peaks of the sulfate ion. And peaks at 1751 cm^{-1}, 1051 cm^{-1} and 1448 cm^{-1} can be

14   assigned to vibrating mode of OA, HSO$_4^-$ ion ($v_s(SO_3)$) and HC$_2$O$_4^-$ ion, respectively. At 75.0% RH,

15   a new peak at 874 cm^{-1} corresponding to the vibrational mode (δ(S-OH)) of HSO$_4^-$ and the HC$_2$O$_4^-$

16   ion vibrating as well as the new peaks at 494, 1469 and 1677 cm^{-1} due to the HC$_2$O$_4^-$ vibrating

17   mode, indicates that crystalline NH$_4$HC$_2$O$_4$ is generated from the reaction of OA with AS. As the

18   RH further decreases to 44.3%, the $v_s(SO_4^{2-})$ band shifts from 979 cm^{-1} to 974 cm^{-1}, and the sharp

19   and narrow bands at 450 and 3126 cm^{-1} appear, indicating the formation of crystallized AS particles.

20   For the mixed OA/AS droplets (OIR = 3:1, Fig. 2c) at 95.9% RH, the bands at 980 cm^{-1}, 1752

21   cm^{-1} and 1050 cm^{-1} are characteristic peak of the sulfate ion, OA and HSO$_4^-$ ion ($v_s(SO_3)$),

22   respectively. And peaks at 1382 and 1460 cm^{-1} can be attributed to vibrating mode of HC$_2$O$_4^-$ ion.

23   When the RH decreases to 74.4%, a new band at 874 cm^{-1} could be assigned to the vibrational mode

24   (δ(S-OH)) of HSO$_4^-$ and the HC$_2$O$_4^-$ ion vibrating. Meanwhile, the bands at 494, 1471 and 1654

25   cm^{-1} can be attributed to HC$_2$O$_4^-$ vibrating mode, suggesting OA reacts with AS to yield crystalline

26   NH$_4$HC$_2$O$_4$ during the dehydration process. At 64.4% RH, the peaks at 494, 874, 1471, 1654, 1718

27   cm^{-1}, and the peak at 3426 cm^{-1} from oxalic acid dihydrate become sharp and narrow, indicating that

28   the OA/AS droplets (OIR = 3:1) completely crystallize to form NH$_4$HSO$_4$, NH$_4$HC$_2$O$_4$ and

29   H$_2$C$_2$O$_4$ 2H$_2$O concurrently. No change in the position and shape of the bands is observed with RH

30   decreasing from 64.4% to 1.1%. Besides the formation of crystalline NH$_4$HSO$_4$ and NH$_4$HC$_2$O$_4$

Atmospheric
Chemistry
and Physics
Discussions

1   during the dehydration process, the mixed droplets crystallize to form $H_2C_2O_4 \cdot 2H_2O$ due to a

2   relatively large amount of OA in the mixed OA/AS droplets (OIR = 3:1).

3   **3.3 Hygroscopicity of pure AS, OA and OA/AS mixtures**

4   **3.3.1 Phase transitions and chemical transformation of AS in mixed systems**

5   Considering that the peak position is sensitive to the chemical environment in the aerosols, the

6   position of the $v_s(SO_4^{2-})$ mode can be used to determine the phase transitions of AS. Figure 3

7   presents the peak position of the $v_s(SO_4^{2-})$ for AS droplets and mixed OA/AS droplets during the

8   dehydration and hydration process, respectively. During the dehydration process, a red shift from

9   979 to 974 cm^{-1} can be observed for AS and OA/AS mixed particles with OIRs of 1:3 and 1:1,

10   indicating crystallization of AS from droplets. During the hydration process, the observations of

11   blue shift from 974 to 979 cm^{-1} for AS and OA/AS mixed particles with OIRs of 1:3 and 1:1

12   suggest the deliquescence transition of AS from crystal phase to aqueous solution. For OA/AS

13   mixed particles with OIRs of 3:1, the peak shift between ~966 and ~979 cm^{-1} is determined during

14   the whole RH cycle. The DRH and ERH for pure and mixed systems have been shown in Fig. 3 and

15   detailed discussion is given in the following section.

16   The peaks at ~1049 and ~979 cm^{-1} for mixed OA/AS droplets (OIRs = 1:3, 1:1 and 3:1) can be

17   attributed to the HSO_4^- and SO_4^{2-} stretching mode, respectively. The area ratio of Raman peaks

18   assigned to the HSO_4^- and SO_4^{2-} is used to indicate the degree of conversion of SO_4^{2-} into HSO_4^- in

19   mixtures, which can be expressed as following:

20   $$\alpha_{HSO_4^-} = A_{1049} / (A_{1049} + A_{979}) \tag{2}$$

21   where A_{1049} and A_{979} is the peak area of the HSO_4^- and SO_4^{2-}, respectively. The ~1049 cm^{-1} for

22   HSO_4^- at solid mixture is not obvious compared to that for solutions. Thus, the calculations are

23   based on the bands at RH approaching full efflorescence point. The estimated α_{HSO4-} value for

24   OIR=1:3 (36.1% RH), OIR=1:1 (46.2% RH) and OIR=3:1 (66.2% RH) is 0.048, 0.368 and 0.644,

25   respectively, indicating the enhanced conversion of SO_4^{2-} into HSO_4^- with increasing OA content in

26   the mixed systems. Due to the effects of Raman cross section, α_{HSO4-} could not represent the actual

27   degree of conversion. In fact, here α_{HSO4-} is only used for comparisons of degree of conversion of

28   SO_4^{2-} into HSO_4^- between mixed particles with varying OIRs.

29   **3.3.2 Hygroscopic growth of pure and mixed components**

30   Hygroscopicity curves of AS and OA particles are shown in Fig. 4. The ERH of AS is determined to

Atmospheric
Chemistry
and Physics
Discussions

1   be 44.3 ± 2.5% RH, which generally falls into the range from 33 to 52% RH reported in the

2   literature (Tang and Munkelwitz, 1994a; Cziczo et al., 1997; Dougle et al., 1998; Dong et al., 2007;

3   Laskina et al., 2015). The DRH of AS particles is observed to occur at 80.1 ± 1.5% RH, which

4   agrees well with reported values of 80% RH by EDB (Tang and Munkelwitz, 1994a) and 82.3 ±

5   2.5% RH by micro-Raman spectroscopy (Laskina et al., 2015). As shown in Fig. 4b, the measured

6   ERH of OA is 77 ± 2.5% RH, which deviates much from the reported value of 51.8-56.7% RH by

7   Peng et al. (2001) using EDB technology. It is worthwhile to point out that the conversion of OA

8   droplets to oxalic acid dihydrate at 77% RH is inconsistent with the observation of Peng et al.

9   (2001). They observed that OA droplets crystallized to form anhydrous oxalic acid rather than

10   oxalic acid dihydrate at 51.8-56.7% RH. The discrepancies between this study and that by Peng et

11   al. (2001) is likely due to the effects of droplet size, substrate and experimental method. According

12   to classical nucleation theory, the probability of the formation of the critical nucleus is proportional

13   to the particle volume (Martin, 2000; Parsons et al., 2006). Considering that the droplet size in our

14   study was approximately 1-2 times larger than that observed by Peng et al. (2001), the droplets

15   deposited on the substrate in our experiment may promote the heterogeneous nucleation while the

16   levitated droplets using EDB can dispel the heterogeneous nucleation. Thus, the ERH of OA

17   obtained in our study is higher than the observation of Peng et al. (2001). The water content of the

18   supersaturated droplet at the onset of crystallization determines the form of oxalic acid crystal

19   generated, i. e., anhydrous OA or OA dihydrate. Due to a higher ERH, oxalic acid droplets with

20   more water content favor the formation of a dihydrate after crystallization. It should be noted that

21   our experiment appears to be favored in the atmospheric environment, considering that insoluble

22   material such as mineral dust mixed with OA may play the role of substrate thus facilitating the

23   heterogeneous nucleation of OA aerosols. The Raman growth factor of OA shows no obvious

24   change between ~77% and 6.6% RH upon dehydration. At RH lower than 5%, the Raman growth

25   factors drop abruptly due to the transformation of crystalline $H_2C_2O_4$ $2H_2O$ into anhydrous oxalic

26   acid, as also indicated by Raman spectrum. During the hydration process, the Raman growth factor

27   of OA shows a slightly increase at 19.6% RH, which can be attributed to the conversion of

28   anhydrous oxalic acid to oxalic acid dihydrate. The transition point of anhydrous oxalic acid to

29   oxalic acid dihydrate agrees with previous studies (Braban et al., 2003; Ma et al., 2013b;

30   Miñambres et al., 2013). No deliquescence behavior is observed for oxalic acid dihydrate even at

Atmospheric
Chemistry
and Physics
Discussions

1 94% RH, consistent with early observations (Ma et al., 2013b; Miñambres et al., 2013; Jing et al.,

2 2016).

3 Figure 5 presents hygroscopic growth of OA/AS mixtures with OIRs of 1:3, 1:1 and 3:1. As can

4 be seen in Fig. 5a, mixed OA/AS droplets (OIR=1:3) exhibit efflorescence transition at lower 34.4 $\pm$

5 2.0% RH relative to ERH (44.3 $\pm$ 2.5%) of pure AS. During the hydration process, mixed particles

6 start to absorb slight water before deliquescence at 81.1 $\pm$ 1.5% RH. The decrease in ERH and

7 slight water uptake before deliquescence for 1:3 mixed particles is likely due to the effects of

8 NH_4HSO_4 formed upon dehydration. NH_4HSO_4 has a low ERH (22-0.05%) and DRH (40%) (Tang

9 and Munkelwitz, 1994a), which may affect the nucleation and crystallization of AS upon

10 dehydration and lead to water uptake before deliquescence of AS. The hygroscopic growth of mixed

11 particles upon dehydration is in fair agreement with that of pure AS or OA. However, the Raman

12 growth factors of mixed particles upon hydration show a considerable decrease in comparison to

13 that upon dehydration. The discrepancies for Raman growth factor at high RH between the two

14 processes can be attributed to the formation of $NH_4HC_2O_4$, which has a high deliquescence point

15 larger than 95% RH (Schroeder and Beyer, 2016). During the hydration process, $NH_4HC_2O_4$ in the

16 mixed aerosols remains solid even at high RH, resulting in less water uptake of mixed particles. The

17 similar phenomenon is also observed for NaCl/OA mixed particles upon hydration due to the

18 formation of less hygroscopic sodium oxalate (Peng et al., 2016).

19 The mixed OA/AS droplets with OIR = 1:1 first partially effloresce at 75.0% $\pm$ 1.6% due to the

20 crystallization of $NH_4HC_2O_4$, as indicated by Raman spectra. Then, the full efflorescence occurs at

21 44.3 $\pm$ 2.5% RH with the crystallization of AS. The full ERH of 1:1 OA/AS mixed droplets is

22 highly consistent with that of pure AS. During the hydration process, the Raman growth factor of

23 1:1 mixed particles increases slightly at 35.5% RH, and then remains almost invariable until 77%

24 RH, which is likely due to the formation of hydrate. The deliquescence transition occurs at 77 $\pm$

25 1.0% RH slightly lower than DRH of AS, which agrees with literature results for AS particles

26 containing OA (Brooks et al., 2002; Jing et al., 2016). The water contents of mixed droplets after

27 deliquescence are significantly lower than those upon dehydration. The Raman features at 494 cm^{-1}

28 and 874 cm^{-1} have confirmed the presence of solid $NH_4HC_2O_4$ upon hydration across all RHs

29 studied (seen in Fig. S2), which should be responsible for the decreasing water uptake of the mixed

30 particles at high RH.

Atmospheric
Chemistry
and Physics
Discussions

1   For mixed OA/AS droplets with OIR = 3:1, the partial and full efflorescence transition could be

2   observed at 74.4 ± 1.0% RH and 64.4 ± 3.0% RH, respectively. As seen in Fig. 2c, the bands at 494,

3   1471 and 1654 cm^{-1} suggest the formation of crystalline $NH_4HC_2O_4$ at 74.4 ± 1.0% RH. The

4   crystallization of $NH_4HC_2O_4$ may act as crystallization nuclei for NH_4^+, HSO_4^- and OA in the mixed

5   droplets to form NH_4HSO_4 crystal and oxalic acid dihydrate. Thus, the full ERH of 3:1 OA/AS

6   mixed droplets is higher than that of pure AS (44.3 ± 2.5% RH) and NH_4HSO_4 (22-0.05% RH).

7   During the hydration process, Raman growth factors of mixed particles slightly increase at 34.5%

8   RH. No deliquescence transition or significant water uptake is observed over the RH range studied.

9   This phenomenon can be explained by the fact that the most of AS in the mixtures has been

10   converted into $NH_4HC_2O_4$ and NH_4HSO_4. Although NH_4HSO_4 with a low DRH may contributes to

11   water uptake of mixed particles, the minor NH_4HSO_4 formed in the mixtures is likely to be coated

12   by $NH_4HC_2O_4$ and OA with a high DRH. Thus, the mixed OA/AS particles with OIR = 3:1 show no

13   obvious hygroscopic growth upon hydration due to the change in aerosol composition and

14   morphology effects. The effects of morphology on the hygroscopic growth of aerosols have been

15   reported for AS particles containing adipic acid (Sjogren et al., 2007). The water uptake of AS

16   particles containing relatively high content of adipic acid could be suppressed due to AS enclosed

17   by the crust of solid adipic acid with a high DRH.

18   The effects of OA on deliquescence behavior of AS has been widely studied. Our results are

19   consistent with early observations that OA had no obvious effects on the DRH of AS in the OA/AS

20   mixtures with a low ratio of OA (Brooks et al., 2002; Wise et al., 2003; Prenni et al., 2003). Prenni

21   et al. (2003) and Miñambres et al. (2013) observed that the equal mass AS/OA mixed particles

22   exhibited a continuous hygroscopic growth through the humidity range studied due to oxalic acid in

23   an amorphous state at low RH. The previous HTDMA studies for equal mass OA/AS mixed

24   particles found that water uptake upon hydration at high RH could be well described by the model

25   methods based on assumption of no composition change, suggesting no specific interactions exist

26   between oxalic acid and ammonium sulfate. However, it should be noted that the total residence

27   time for transformation of droplets into dry particles in the drying section of HTDMA is typically

28   tens of seconds (Kumar et al., 2003; Prenni et al., 2003; Jing et al., 2016; Peng et al., 2016), much

29   shorter than that (10 ~ 12 h) in our study. Considering the potential effects of drying time on the

30   reactions between OA and AS, we explored the hygroscopicity of OA/AS particles with OIR of 1:1

Atmospheric
Chemistry
and Physics
Discussions

1   after rapid drying process. The mixed OA/AS droplets undergo dehydration to form dry particles in

2   3 ~ 5 min. The Raman spectra and hygroscopic curve upon hydration for OA/AS particles with OIR

3   of 1:1 are presented in Fig. 6. The obvious discrepancies can be observed for spectra at ~2% RH

4   between the two drying processes. After rapid drying process, the spectra at ~2% RH show the

5   feature of crystalline AS (967 cm^{-1}, ν_s(SO$_4^{2-}$)) and anhydrous OA (1710 cm^{-1}, ν(C=O); 1479 cm^{-1},

6   ν_s(COO)). Meanwhile, no characteristic peaks for NH$_4$HC$_2$O$_4$ (494 cm^{-1}, δ(COO); 874 cm^{-1}, ν(C-C);

7   1729 cm^{-1}, ν(C=O); 1469 cm^{-1}, ν_s(COO)) and NH$_4$HSO$_4$ (874 cm^{-1}, δ(S-OH)) can be identified in

8   the spectra. It is clear that the drying time for transformation of droplets into dry particles has

9   impacts on the reactions of OA with AS in the aerosols due to particle-phase processes under kinetic

10   control. Previous studies found the longer drying time could lead to greater nitrate depletion

11   between nitrates and organic acids, which results from slow reaction and diffusion in the viscous

12   aerosols (Wang and Laskin, 2014). The Raman growth factors of mixed particles with OIR of 1:1

13   also increase slightly at 36.5% RH due to the formation of OA dihydrate, as indicated by the Raman

14   feature. The deliquescence transition of mixed particles occurs at 79.3% RH. After deliquescence,

15   Raman growth factors of mixed particles after rapid drying process are lower than that after slow

16   drying process, which may be caused by the fact that at high RH the hygroscopic growth of AS is

17   slightly lower than that of NH$_4$HSO$_4$ formed in the particles after slow drying process (Tang and

18   Munkelwitz, 1977). In addition, it is found that after deliquescence OA dihydrate remains solid in

19   the mixed particles after rapid drying process.

20   **4 Conclusions**

21   In this work, confocal Raman spectroscopy is used to investigate the hygroscopic properties and

22   phase transformations of OA and internally mixed OA/AS droplets (OIRs = 1:3, 1:1 and 3:1). OA

23   droplets effloresce to form oxalic acid dihydrate at 77 ±2.5% RH, and then oxalic acid dihydrate

24   further loses crystalline water to form anhydrous oxalic acid at ~5.0% RH during the dehydration

25   process. The Raman spectra of mixed OA/AS droplets reveal the formation of NH$_4$HC$_2$O$_4$ and

26   NH$_4$HSO$_4$ from the reaction of OA with AS in aerosols after slow dehydration process. The

27   deliquescence and efflorescence point for AS is observed to occur at 80.1 ±1.5% and 44.3 ±2.5%

28   RH, respectively. The ERH of the mixed OA/AS droplets with 1:3, 1:1 and 3:1 ratio is determined

29   to be 34.4 ±2.0%, 44.3 ±2.5% and 64.4 ±3.0% RH, respectively, indicating significant effects of

30   OA content on the efflorescence transition of AS. The mixed OA/AS particles with 1:3 and 1:1 ratio

Atmospheric
Chemistry
and Physics
Discussions

1   show deliquescence transition at 81.1 ±1.5% and 77 ±1.0% RH, respectively, which is close to the

2   DRH of AS. The mixed OA/AS particles with 3:1 ratio exhibit no deliquescence transition over the

3   RH range studied due to the transformation of $(NH_4)_2SO_4$ into nonhygroscopic $NH_4HC_2O_4$. The

4   hygroscopic growth of mixed particles at high RH upon hydration is substantially lower than that of

5   corresponding dehydration process and further decreases with increasing OA content. The

6   discrepancies for water content of mixed particles between the two processes at high RH can be

7   explained by the significant formation of low hygroscopic $NH_4HC_2O_4$ and residual OA, which still

8   remain solid and thus result in less water uptake of mixed particles.

9   Field and laboratory observations have shown that organic acids can react with inorganic salts

10   within aerosols (Kerminen et al., 1998; Laskin et al., 2012; Laskina et al., 2013; Ma et al., 2013b;

11   Wang and Laskin, 2014; Ghorai et al., 2014; Peng et al., 2016). Ma et al. (2013b) observed that

12   reactions of OA with NaCl upon dehydration resulted in the formation of less hygroscopic disodium

13   oxalate driven by the high volatility of gaseous HCl. Wang and Laskin (2014) reported that the

14   water-soluble organic acids could react with nitrates due to the release of HNO_3 during the

15   dehydration process. Despite no release of high volatile gas (such as HCl and HNO_3), our results

16   reveal that OA can react with AS to form low hygroscopic organic salts in aerosols undergoing slow

17   dehydration process. Our finds highlight the role of drying rate in formation of organic salts from

18   reactions of organic acids with inorganic salts in aerosols under ambient RH conditions. Thus, the

19   drying conditions have potential effects on reactions and composition in aerosols, which have

20   important implications for atmospheric chemistry.

23   **The Supplement related to this article is available online at supplement.**

24   **References**

25   Braban, C. F., Carroll, M. F., Styler, S. A., and Abbatt, J. P. D.: Phase transitions of malonic and

26   oxalic acid aerosols, J. Phys. Chem. A, 107, 6594-6602, doi: 10.1021/jp034483f, 2003.

27   Brooks, S. D., Wise, M. E., Cushing, M., and Tolbert, M. A.: Deliquescence behavior of

28   organic/ammonium sulfate aerosol, Geophys. Res. Lett., 29, 1917, doi: 10.1029/2002gl014733,

29   2002.

Atmospheric
Chemistry
and Physics
Discussions

1　Chang, H., and Huang, P. J.: Thermal decomposition of $CaC_2O_4 \cdot H_2O$ studied by thermo-Raman

2　　spectroscopy with TGA/DTA, Anal. Chem., 69, 1485-1491, doi: 10.1021/ac960881l, 1997.

3　Chebbi, A., and Carlier, P.: Carboxylic acids in the troposphere, occurrence, sources, and sinks: A

4　　review, Atmos. Environ., 30, 4233-4249, doi: 10.1016/1352-2310(96)00102-1, 1996.

5　Colberg, C. A.: Experimente an levitierten $H_2SO_4/NH_3/H_2O$-Aerosolteilchen: Atmosphärische

6　　Relevanz von Letovizit, Ph.D. Dissertation, Swiss federal institute of technology (ETH) Zuerich,

7　　2001.

8　Cziczo, D. J., Nowak, J. B., Hu, J. H., and Abbatt, J. P. D.: Infrared spectroscopy of model

9　　tropospheric aerosols as a function of relative humidity: Observation of deliquescence and

10　　crystallization, J. Geophys. Res., 102, 18843-18850, doi: 10.1029/97jd01361, 1997.

11　Dawson, B. S. W., Irish, D. E., and Toogood, G. E.: Vibrational spectral studies of solutions at

12　　elevated temperatures and pressures. 8. A Raman spectral study of ammonium hydrogen sulfate

13　　solutions and the HSO_4^--SO_4^{2-} equilibrium, J. Phys. Chem., 90, 334-341, doi:

14　　10.1021/j100274a027, 1986.

15　Dong, J. L., Li, X. H., Zhao, L. J., Xiao, H. S., Wang, F., Guo, X., and Zhang, Y. H.: Raman

16　　observation of the interactions between NH_4^+, SO_4^{2-}, and H_2O in supersaturated $(NH_4)_2SO_4$

17　　droplets, J. Phys. Chem. B, 111, 12170-12176, doi: 10.1021/jp072772o, 2007.

18　Dong, J. L., Xiao, H. S., Zhao, L. J., and Zhang, Y. H.: Spatially resolved Raman investigation on

19　　phase separations of mixed $Na_2SO_4/MgSO_4$ droplets, J. Raman Spectrosc., 40, 338-343, doi:

20　　10.1002/jrs.2132, 2009.

21　Dougle, P. G., Veefkind, J. P., and ten Brink, H. M.: Crystallisation of mixtures of ammonium nitrate,

22　　ammonium sulphate and soot, J. Aerosol Sci., 29, 375-386, doi: 10.1016/S0021-8502(97)10003-9,

23　　1998.

24　Drozd, G., Woo, J., Häkkinen, S. A. K., Nenes, A., and McNeill, V. F.: Inorganic salts interact with

25　　oxalic acid in submicron particles to form material with low hygroscopicity and volatility, Atmos.

26　　Chem. Phys., 14, 5205-5215, doi: 10.5194/acp-14-5205-2014, 2014.

27　Ebisuzaki, Y., and Angel, S. M.: Raman study of hydrogen bonding in α and β-oxalic acid dihydrate,

28　　J. Raman Spectrosc., 11, 306-311, doi: 10.1002/jrs.1250110416, 1981.

29　Ghorai, S., Wang, B., Tivanski, A., and Laskin, A.: Hygroscopic properties of internally mixed

30　　particles composed of NaCl and water-soluble organic acids, Environ. Sci. Technol., 48,

Atmospheric
Chemistry
and Physics
Discussions
Open Access
EGU

1   2234-2241, doi: 10.1021/es404727u, 2014.

2   Hibben, J. H.: The Raman Spectra of Oxalic Acid, J. Chem. Phys., 3, 675-679, doi:

3   10.1063/1.1749575, 1935.

4   Irish, D. E., and Chen, H.: Equilibriums and proton transfer in the bisulfate-sulfate system, J. Phys.

5   Chem., 74, 3796-3801, doi: 10.1021/j100715a014, 1970.

6   Jacobson, M. C., Hansson, H. C., Noone, K. J., and Charlson, R. J.: Organic atmospheric aerosols:

7   Review and state of the science, Rev. Geophys., 38, 267-294, doi: 10.1029/1998RG000045,

8   2000.

9   Jing, B., Tong, S. R., Liu, Q. F., Li, K., Wang, W. G., Zhang, Y. H., and Ge, M. F.: Hygroscopic

10   behavior of multicomponent organic aerosols and their internal mixtures with ammonium sulfate,

11   Atmos. Chem. Phys., 16, 4101-4118, 2016.

12   Jing, B., Peng, C., Wang, Y., Liu, Q. F., Tong, S. R., Zhang, Y. H., and Ge, M. F.: Hygroscopic

13   properties of potassium chloride and its internal mixtures with organic compounds relevant to

14   biomass burning aerosol particles, Sci. Rep., 7, 43572, doi: 10.1038/srep43572, 2017.

15   Kanakidou, M., Seinfeld, J. H., Pandis, S. N., Barnes, I., Dentener, F. J., Facchini, M. C., Van

16   Dingenen, R., Ervens, B., Nenes, A., Nielsen, C. J., Swietlicki, E., Putaud, J. P., Balkanski, Y.,

17   Fuzzi, S., Horth, J., Moortgat, G. K., Winterhalter, R., Myhre, C. E. L., Tsigaridis, K., Vignati, E.,

18   Stephanou, E. G., and Wilson, J.: Organic aerosol and global climate modelling: a review, Atmos.

19   Chem. Phys., 5, 1053-1123, doi: 10.5194/acp-5-1053-2005, 2004.

20   Kawamura, K., and Bikkina, S.: A review of dicarboxylic acids and related compounds in

21   atmospheric aerosols: Molecular distributions, sources and transformation, Atmos. Res., 170,

22   140-160, doi: 10.1016/j.atmosres.2015.11.018, 2016.

23   Kerminen, V. M., Teinilä, K., Hillamo, R., and Pakkanen, T.: Substitution of chloride in sea-salt

24   particles by inorganic and organic anions, J. Aerosol Sci., 29, 929-942, doi:

25   10.1016/S0021-8502(98)00002-0, 1998.

26   Kruus, P., Hayes, A. C., and Adams, W. A.: Determination of ratios of sulfate to bisulfate ions in

27   aqueous solutions by raman spectroscopy, J. Solution Chem., 14, 117-128, doi:

28   10.1007/BF00648900, 1985.

29   Kumar, P. P., Broekhuizen, K., and Abbatt, J. P. D.: Organic acids as cloud condensation nuclei:

30   Laboratory studies of highly soluble and insoluble species, Atmos. Chem. Phys., 3, 509–520, doi:

Atmospheric
Chemistry
and Physics
Discussions

1   10.5194/acp-3-509-2003, 2003.

2   Laskin, A., Moffet, R. C., Gilles, M. K., Fast, J. D., Zaveri, R. A., Wang, B., Nigge, P., and

3   Shutthanandan, J.: Tropospheric chemistry of internally mixed sea salt and organic particles:

4   Surprising reactivity of NaCl with weak organic acids, J. Geophys. Res., 117, D15302, doi:

5   10.1029/2012jd017743, 2012.

6   Laskina, O., Young, M. A., Kleiber, P. D., and Grassian, V. H.: Infrared extinction spectroscopy and

7   micro-Raman spectroscopy of select components of mineral dust mixed with organic compounds,

8   J. Geophys. Res., 118, 6593-6606, doi: 10.1002/jgrd.50494, 2013.

9   Laskina, O., Morris, H. S., Grandquist, J. R., Qin, Z., Stone, E. A., Tivanski, A. V., and Grassian, V.

10 H.: Size matters in the water uptake and hygroscopic growth of atmospherically relevant

11 multicomponent aerosol particles, J. Phys. Chem. A, 119, 4489-4497, doi: 10.1021/jp510268p,

12 2015.

13 Li, X., Gupta, D., Lee, J., Park, G., and Ro, C. U.: Real-time investigation of chemical compositions

14 and hygroscopic properties of aerosols generated from NaCl and malonic acid mixture solutions

15 using in situ Raman microspectrometry, Environ. Sci. Technol., 51, 263−270, doi:

16 10.1021/acs.est.6b04356, 2017.

17 Lightstone, J. M., Onasch, T. B., Imre, D., and Oatis, S.: Deliquescence, efflorescence, and water

18 activity in ammonium nitrate and mixed ammonium nitrate/succinic acid microparticles, J. Phys.

19 Chem. A, 104, 9337-9346, doi: 10.1021/jp002137h, 2000.

20 Liu, Y., Yang, Z. W., Desyaterik, Y., Gassman, P. L., Wang, H., and Laskin, A.: Hygroscopic

21 behavior of substrate-deposited particles studied by micro-FT-IR spectroscopy and

22 complementary methods of particle analysis, Anal. Chem., 80, 633–642, doi: 10.1021/ac701638r,

23 2008.

24 Ma, Q., and He, H.: Synergistic effect in the humidifying process of atmospheric relevant calcium

25 nitrate, calcite and oxalic acid mixtures, Atmos. Environ., 50, 97-102, doi:

26 10.1016/j.atmosenv.2011.12.057, 2012.

27 Ma, Q., He, H., and Liu, C.: Hygroscopic properties of oxalic acid and atmospherically relevant

28 oxalates, Atmos. Environ., 69, 281-288, doi: 10.1016/j.atmosenv.2012.12.011, 2013a.

29 Ma, Q., Ma, J., Liu, C., Lai, C., and He, H.: Laboratory study on the hygroscopic behavior of

30 external and internal C_2-C_4 dicarboxylic acid-NaCl mixtures, Environ. Sci. Technol., 47,

Atmospheric
Chemistry
and Physics
Discussions

1   10381-10388, doi: 10.1021/es4023267, 2013b.

2   Martin, S. T.: Phase transitions of aqueous atmospheric particles, Chem. Rev., 100, 3403-3454, doi:

3   10.1021/cr990034t, 2000.

4   Miñambres, L., Méndez, E., Sánchez, M. N., Castaño, F., and Basterretxea, F. J.: Water uptake of

5   internally mixed ammonium sulfate and dicarboxylic acid particles probed by infrared

6   spectroscopy, Atmos. Environ., 70, 108-116, doi: 10.1016/j.atmosenv.2013.01.007, 2013.

7   Mikhailov, E., Vlasenko, S., Martin, S. T., Koop, T., and Pöschl, U.: Amorphous and crystalline

8   aerosol particles interacting with water vapor: conceptual framework and experimental evidence

9   for restructuring, phase transitions and kinetic limitations, Atmos. Chem. Phys., 9 9491–9522,

10   2009.

11   Mohaček-Grošev, V., Grdadolnik, J., Stare, J., and Hadži, D.: Identification of hydrogen bond

12   modes in polarized Raman spectra of single crystals of α-oxalic acid dihydrate, J. Raman

13   Spectrosc., 40, 1605-1614, doi: 10.1002/jrs.2308, 2009.

14   Murphy, D. M., Thomson, D. S., and Mahoney, M. J.: In situ measurements of organics, meteoritic

15   material, mercury, and other elements in aerosols at 5 to 19 kilometers, Science, 282, 1664-1669,

16   doi: 10.1126/science.282.5394.1664, 1998.

17   Murphy, D. M., Cziczo, D. J., Froyd, K. D., Hudson, P. K., Matthew, B. M., Middlebrook, A. M.,

18   Peltier, R. E., Sullivan, A., Thomson, D. S., and Weber, R. J.: Single-particle mass spectrometry

19   of tropospheric aerosol particles, J. Geophys. Res., 111, D23S32, doi: 10.1029/2006JD007340,

20   2006.

21   Pöschl, U.: Atmospheric aerosols: composition, transformation, climate and health effects, Angew.

22   Chem. Int. Ed., 44, 7520-7540, 2005.

23   Parsons, M. T., Riffell, J. L., and Bertram, A. K.: Crystallization of aqueous inorganic-malonic acid

24   particles: Nucleation rates, dependence on size, and dependence on the ammonium-to-sulfate

25   ratio, J. Phys. Chem. A, 110, 8108-8115, doi: 10.1021/jp057074n, 2006.

26   Peng, C., Jing, B., Guo, Y. C., Zhang, Y. H., and Ge, M. F.: Hygroscopic Behavior of

27   Multicomponent Aerosols Involving NaCl and Dicarboxylic Acids, J. Phys. Chem. A, 120,

28   1029-1038, doi: 10.1021/acs.jpca.5b09373, 2016.

29   Peng, C. G., Chan, M. N., and Chan, C. K.: The hygroscopic properties of dicarboxylic and

30   multifunctional acids: Measurements and UNIFAC predictions, Environ. Sci. Technol., 35,

Atmospheric
Chemistry
and Physics
Discussions

1 4495-4501, doi: 10.1021/es0107531, 2001.

2 Penner, J. E., Andreae, M. O., Annegarn, H., Barrie, L., Feichter, J., Hegg, D., Jayaraman, A.,

3   Leaitch, R., Murphy, D., Nganga, J., and Pitari, G.: Aerosols, their direct and indirect effects, in:

4   Climate Change 2001: The Scientific Basis. Contribution of Working Group I to the Third

5   Assessment Report of the Intergovernmental Panel on Climate Change, Cambridge University

6   Press, 289-348, 2001.

7 Pratt, K. A., and Prather, K. A.: Aircraft measurements of vertical profiles of aerosol mixing states, J.

8   Geophys. Res., 115, D11305, doi: 10.1029/2009JD013150, 2010.

9 Prenni, A. J., DeMott, P. J., and Kreidenweis, S. M.: Water uptake of internally mixed particles

10   containing ammonium sulfate and dicarboxylic acids, Atmos. Environ., 37, 4243–4251, doi:

11   10.1016/S1352-2310(03)00559-4, 2003.

12 Saxena, P., Hildemann, L. M., Mcmurry, P. H., and Seinfeld, J. H.: Organics alter hygroscopic

13   behavior of atmospheric particles, J. Geophys. Res., 100, 18755-18770, doi: 10.1029/95JD01835,

14   1995.

15 Schroeder, J. R., and Beyer, K. D.: Deliquescence relative humidities of organic and inorganic salts

16   important in the atmosphere, J. Phys. Chem. A, 120, 9948–9957, doi: 10.1021/acs.jpca.6b08725,

17   2016.

18 Shippey, T. A.: Very strong hydrogen bonding: single crystal raman studies of potassium hydrogen

19   oxalate and sodium hydrogen oxalate monohydrate, J. Mol. Struct., 57, l-11, doi:

20   10.1016/0022-2860(79)80227-6, 1979.

21 Sjogren, S., Gysel, M., Weingartner, E., Baltensperger, U., Cubison, M. J., Coe, H., Zardini, A. A.,

22   Marcolli, C., Krieger, U. K., and Peter, T.: Hygroscopic growth and water uptake kinetics of

23   two-phase aerosol particles consisting of ammonium sulfate, adipic and humic acid mixtures, J.

24   Aerosol Sci., 38, 157-171, doi: 10.1016/j.jaerosci.2006.11.005, 2007.

25 Spinner, E.: Raman-spectral depolarisation ratios of ions in concentrated aqueous solution. The

26   next-to-negligible effect of highly asymmetric ion surroundings on the symmetry properties of

27   polarisability changes during vibrations of symmetric ions. Ammonium sulphate and

28   tetramethylammonium bromide, Spectrochim. Acta, Part A, 59, 1441-1456, doi:

29   10.1016/s1386-1425(02)00293-7, 2003.

30 Tang, I. N., and Munkelwitz, H. R.: Aerosol growth studies—III ammonium bisulfate aerosols in a

Atmospheric
Chemistry
and Physics
Discussions

1   moist atmosphere, J. Aerosol Sci., 8, 321-330, 1977.

2   Tang, I. N., and Munkelwitz, H. R.: Water activities, densities, and refractive indices of aqueous

3   sulfates and sodium nitrate droplets of atmospheric importance, J. Geophys. Res., 99,

4   18801-18808, doi: 10.1029/94JD01345, 1994a.

5   Tang, I. N., and Munkelwitz, H. R.: Aerosol phase-transformation and growth in the atmosphere, J.

6   Appl. Meteorol., 33, 791-796, doi: 10.1175/1520-0450(1994)033<0791:Aptagi>2.0.Co;2, 1994b.

7   Treuel, L., Sandmann, A., and Zellner, R.: Spatial separation of individual substances in effloresced

8   crystals of ternary ammonium sulphate/dicarboxylic acid/water aerosols, ChemPhysChem, 12,

9   1109-1117, doi: 10.1002/cphc.201000738, 2011.

10   Villepin, J. D., and Novak, A.: Vibrational spectra of and isotope effect in hydrogen bonded

11   potassium hydrogen oxalate, Spectrosc. Lett., 4, 1-8, doi: 10.1080/00387017108078634, 1971.

12   Von Schneidemesser, E., Monks, P. S., Allan, J. D., Bruhwiler, L., Forster, P., Fowler, D., Lauer, A.,

13   Morgan, W. T., Paasonen, P., Righi, M., Sindelarova, K., and Sutton, M. A.: Chemistry and the

14   linkages between air quality and climate change, Chem. Rev., 115, 3856-3897, 2015.

15   Wang, B., and Laskin, A.: Reactions between water-soluble organic acids and nitrates in

16   atmospheric aerosols: Recycling of nitric acid and formation of organic salts, J. Geophys. Res.,

17   119, 3335-3351, doi: 10.1002/2013jd021169, 2014.

18   Wang, F., Zhang, Y. H., Zhao, L. J., Zhang, H., Cheng, H., and Shou, J. J.: Micro-Raman study on

19   the conformation behavior of succinate in supersaturated sodium succinate aerosols, Phys. Chem.

20   Chem. Phys., 10, 4154-4158, doi: 10.1039/b719457a, 2008.

21   Wang, G. H., Kawamura, K., Cheng, C. L., Li, J. J., Cao, J. J., Zhang, R. J., Zhang, T., Liu, S. X.,

22   and Zhao, Z. Z.: Molecular distribution and stable carbon isotopic composition of dicarboxylic

23   acids, ketocarboxylic acids, and α-dicarbonyls in size-resolved atmospheric particles from Xi'an

24   City, China, Environ. Sci. Technol., 46, 4783-4791, doi: 10.1021/es204322c, 2012.

25   Wang, Y., Ma, J. B., Zhou, Q., Pang, S. F., and Zhang, Y. H.: Hygroscopicity of mixed

26   glycerol/$Mg(NO_3)_2$/water droplets affected by the interaction between magnesium ions and

27   glycerol molecules, J. Phys. Chem. B, 119, 5558-5566, doi: 10.1021/acs.jpcb.5b00458, 2015.

28   Wise, M. E., Surratt, J. D., Curtis, D. B., Shilling, J. E., and Tolbert, M. A.: Hygroscopic growth of

29   ammonium sulfate/dicarboxylic acids, J. Geophys. Res., 108, 4638, doi: 10.1029/2003jd003775,

30   2003.

Atmospheric
Chemistry
and Physics
Discussions

1 Yang, L., and Yu, L. E.: Measurements of oxalic acid, oxalates, malonic acid, and malonates in

2 atmospheric particulates, Environ. Sci. Technol., 42, 9268-9275, 2008.

3 Yu, J. Y., Zhang, Y., Zeng, G., Zheng, C. M., Liu, Y., and Zhang, Y. H.: Suppression of $NaNO_3$

4 crystal nucleation by glycerol: micro-Raman observation on the efflorescence process of mixed

5 glycerol/$NaNO_3$/water droplets, J. Phys. Chem. B, 116, 1642-1650, doi: 10.1021/jp210824e,

6 2012.

7 Zhou, Q., Pang, S. F., Wang, Y., Ma, J. B., and Zhang, Y. H.: Confocal Raman studies of the

8 evolution of the physical state of mixed phthalic acid/ammonium sulfate aerosol droplets and the

9 effect of substrates, J. Phys. Chem. B, 118, 6198-6205, doi: 10.1021/jp5004598, 2014.

10

11

Atmospheric
Chemistry
and Physics
Discussions

Table 1. Molecular vibration assignments of pure oxalic acid and ammonium sulfate.

Solid $H_2C_2O_4$		$H_2C_2O_4$	$(NH_4)_2SO_4$		
Anhydrous	Dihydrate	Droplets (92.5% RH)	Droplets (94.8% RH)	Refs	Assignments
			450	(Spinner, 2003; Colberg, 2001; Dong et al., 2007)	$\delta_s(SO_4^{2-})$
482	477	457		(Hibben, 1935; Ebisuzaki and Angel, 1981)	$\delta(OCO)$
828				(Ebisuzaki and Angel, 1981)	$r(OCO)$
845	855	845		(Ma et al., 2013a; Ebisuzaki and Angel, 1981)	$v(C\text{-}C)$
			979	(Spinner, 2003; Colberg, 2001; Dong et al., 2007)	$v_s(SO_4^{2-})$
1477	1490	1460		(Ma et al., 2013a; Ebisuzaki and Angel, 1981)	$v_s(COO)$
	1627	1636		(Ma et al., 2013a; Ebisuzaki and Angel, 1981)	$\delta(HOH)$
	1689			(Ma et al., 2013a; Ebisuzaki and Angel, 1981)	$v(C{=}O)$
1710	1737	1750		(Ma et al., 2013a; Ebisuzaki and Angel, 1981)	$v(C{=}O)$
2587, 2760				(Mohaček-Grošev et al., 2009)	Combinations
2909					
			3080	(Spinner, 2003; Colberg, 2001; Dong et al., 2007)	Combinations
			3240	(Spinner, 2003; Colberg, 2001; Dong et al., 2007)	$v(OH)$
	3433,3474	3433	3437	(Spinner, 2003; Dong et al., 2007; Colberg, 2001)	$v(OH)$

v: stretching; δ: bending; r: rocking; s: symmetric mode.

Atmospheric
Chemistry
and Physics
Discussions

Table 2. Molecular vibration assignments of mixed OA/AS systems

$H_2C_2O_4$-$(NH_4)_2SO_4$ (1:3), RH=96.2%	$H_2C_2O_4$-$(NH_4)_2SO_4$ (1:1), RH=96.1%	$H_2C_2O_4$-$(NH_4)_2SO_4$ (3:1), RH=95.9%	Refs	Assignments
450	450	461	(Spinner, 2003; Colberg, 2001; Dong et al., 2007)	$\delta_s(SO_4^{2-})$
	852	850	(Ebisuzaki and Angel, 1981; Ma et al., 2013a)	$\nu(C\text{-}C)$
979	979	980	(Spinner, 2003; Dong et al., 2007; Colberg, 2001)	$\nu_s(SO_4^{2-})$
1049	1051	1050	(Irish and Chen, 1970; Kruus et al., 1985; Dawson et al., 1986)	$\nu_s(SO_3)$
	1382	1382	(Ma et al., 2013a; Chang and Huang, 1997)	$\omega(OCO)$
1446	1448	1460	(Hibben, 1935; Ebisuzaki and Angel, 1981; Ma et al., 2013a)	$\nu_s(COO)$
1694			(Ma et al., 2013a; Ebisuzaki and Angel, 1981)	$\nu(C\text{=}O)$
1741	1751	1752	(Ma et al., 2013a; Ebisuzaki and Angel, 1981)	$\nu(C\text{=}O)$
3430	3427	3426	(Spinner, 2003; Dong et al., 2007; Colberg, 2001)	$\nu(OH)$

ν: stretching; δ: bending; ω: wagging; s: symmetric mode.

Atmospheric
Chemistry
and Physics
Discussions
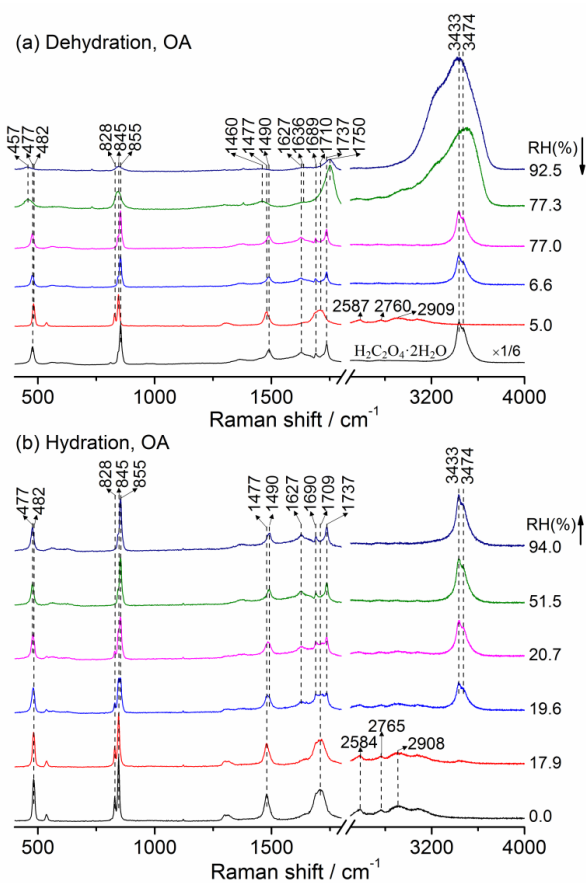
Figure 1. Raman spectra of OA droplets during the (a) dehydration process and (b) hydration process. In panel (a), the peak height of ν(OH) of $H_2C_2O_4$ $2H_2O$ particles located at 3433 cm^{-1} is scaled by a factor of 1/6.

Atmospheric
Chemistry
and Physics
Discussions

1
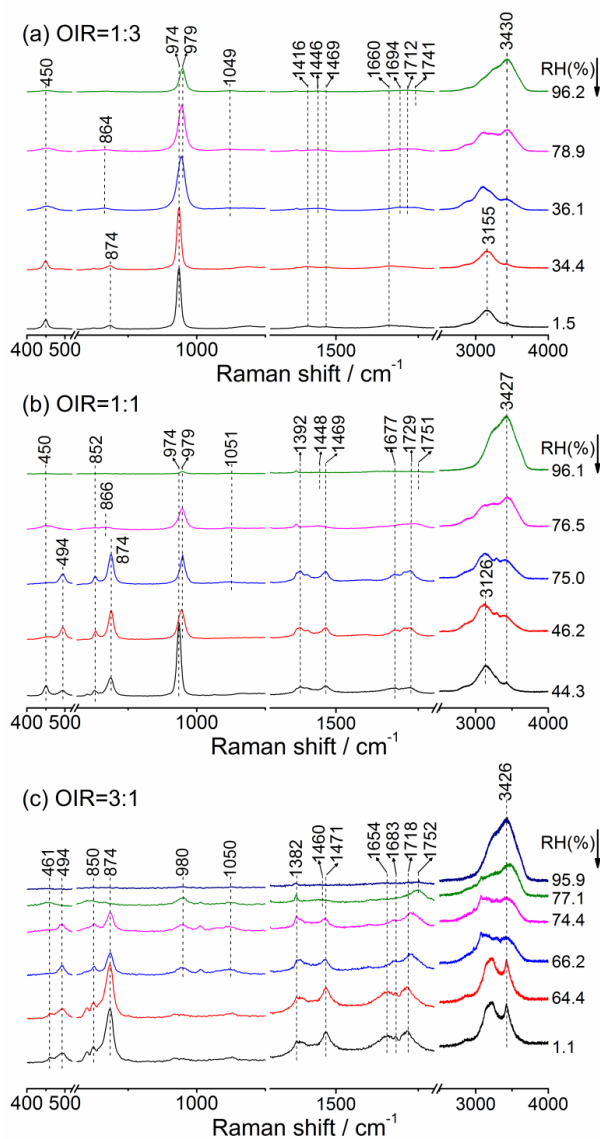
Figure 2. Raman spectra of mixed OA/AS droplets with OIRs of (a) 1:3 (b) 1:1 (c) 3:1 at various

3   RH values during the dehydration process.

4

1
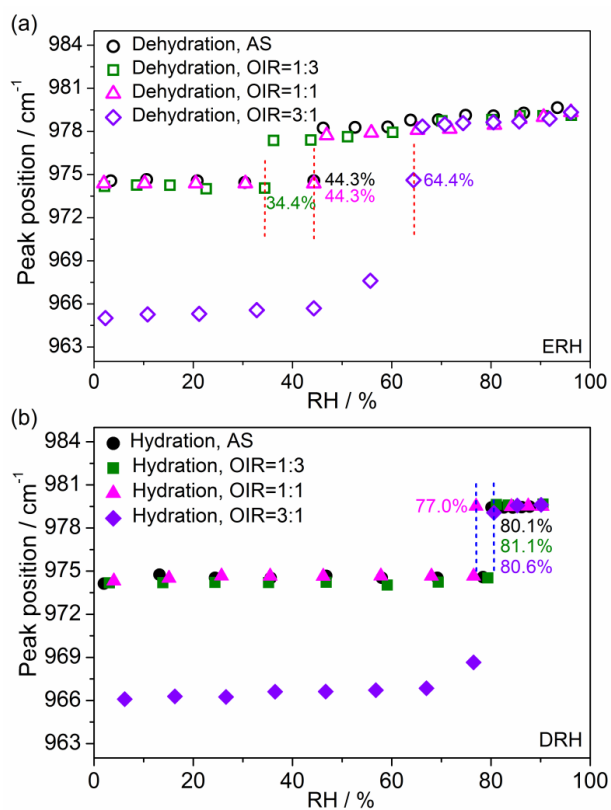
Figure 3. The peak position of the ν_1-SO_4^{2-} peak of mixed OA/AS particles and pure AS particles at

various RHs during the (a) dehydration and (b) hydration process. The red and blue dashed lines

indicate the ERH and DRH, respectively.

5

Atmospheric
Chemistry
and Physics
Discussions

Open Access

1
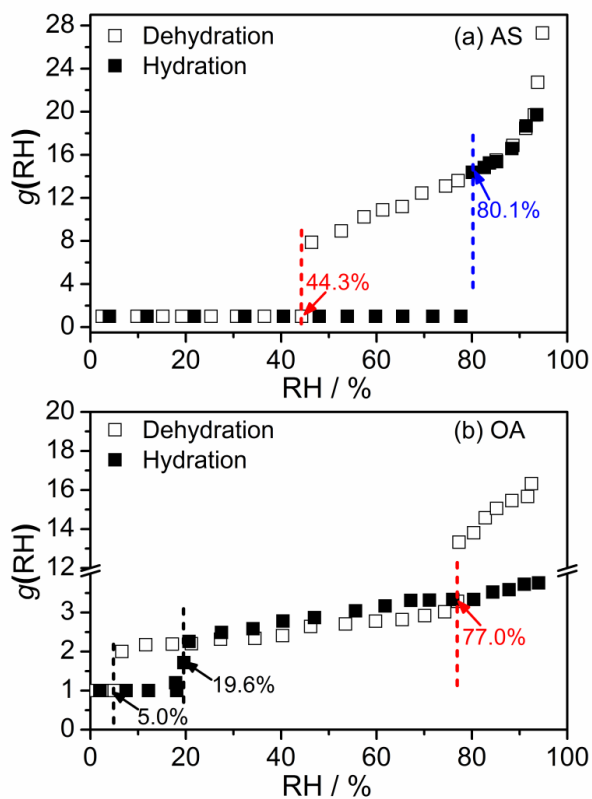
Figure 4. Hygroscopicity of (a) AS and (b) OA as a function of RH by Raman spectroscopy. The
red and blue dashed lines indicate the ERH and DRH, respectively. The black lines show phase
transition point for the transformation between oxalic acid dihydrate and anhydrous oxalic acid.

5

Atmospheric
Chemistry
and Physics
Discussions

Open Access

EGU

1
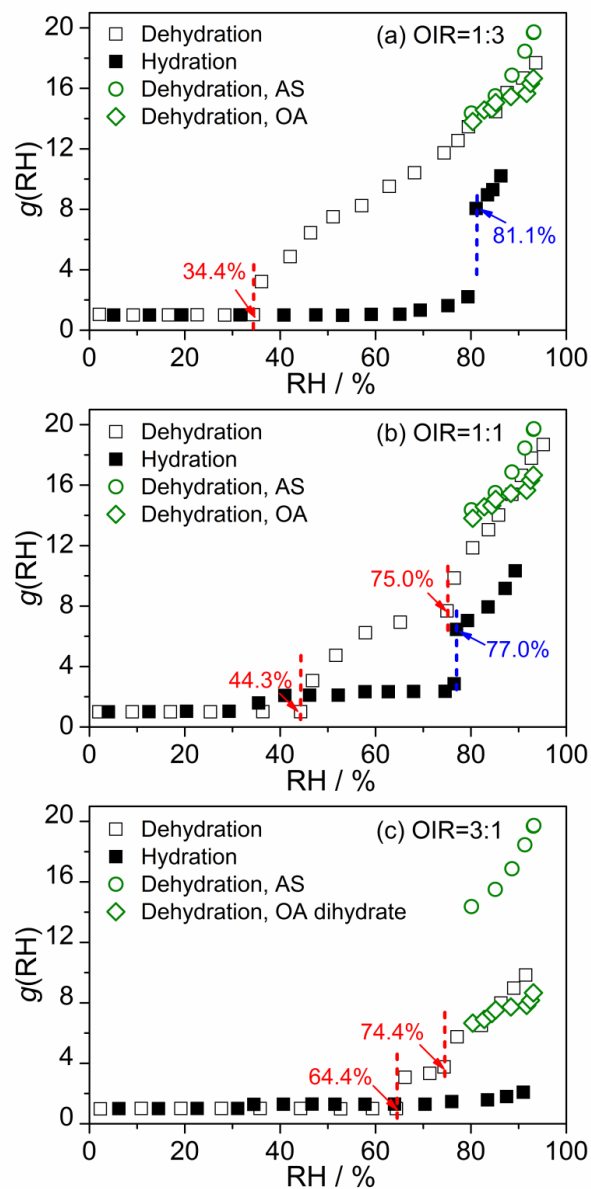
Figure 5. Hygroscopicity of OA/AS mixtures with OIRs of (a) 1:3, (b) 1:1 and (c) 3:1 as a function

of RH by Raman spectroscopy. The red and blue dashed lines indicate the ERH and DRH,

respectively. In the a and b, Raman growth factors of pure AS and OA above 80% RH in the

dehydration process are also included for comparisons. In the c, Raman growth factors of pure AS

and OA dihydrate above 80% RH during the dehydration process are also given for comparisons.

7

Atmospheric
Chemistry
and Physics
Discussions

1

2

3
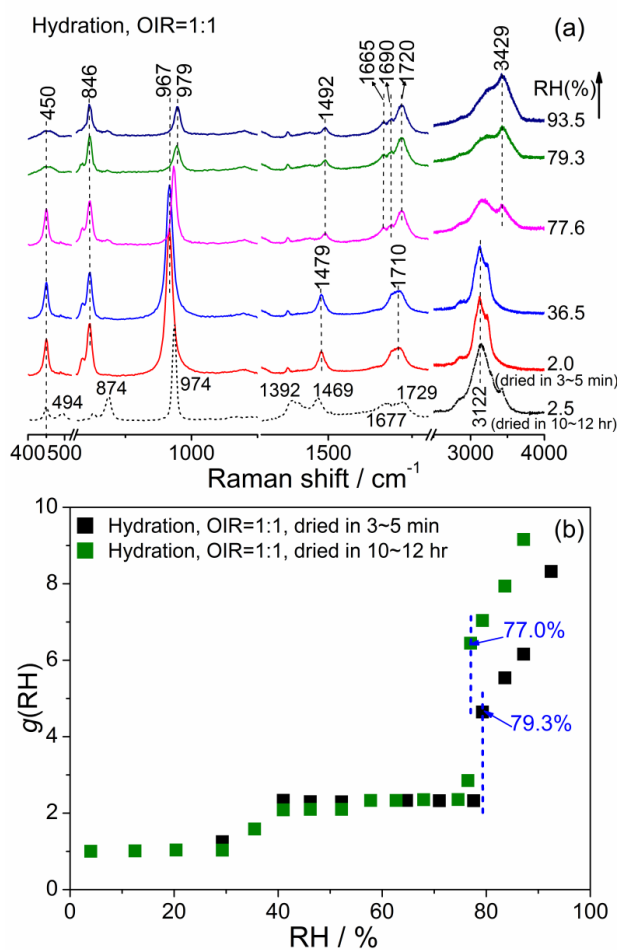
Figure 6. (a) Raman spectra of equal molar mixed OA/AS particles after rapid drying process at

various RH values upon hydration. The Raman spectrum (black short dash) at 2.5% RH obtained

from the slow drying process is also given for comparisons. (b) Deliquescence curve of OA/AS

mixtures with OIR of 1:1. The hygroscopic curve (olive line) of particles after slow drying process

is also included for comparisons. The blue dashed lines indicate the DRH.

9